

Research on Photo-Varistor Based on Lateral Bipolar Photoresistance Effect

Mingjun Gao

Abstract: Previous studies have investigated the bipolar resistance effect in various semiconductor materials, suggesting the potential for developing a new type of photoresistive device based on this effect. However, further research and optimization of the fabrication process for such photoresistive devices are still needed. This project focuses on the in-depth study of the fabrication process for this type of photoresistive device. Firstly, a series of experiments were conducted to select two semiconductor materials with good linearity: one is P-type silicon (Ag/SiO₂/Si) corroded for 10 minutes, and the other is N-type silicon (Ag/SiO₂/Si) corroded for 5 minutes. Subsequently, other components were fabricated using 3D printing technology, and these components were combined with the selected silicon pieces to create resistors with different sensitivities. Furthermore, an Arduino circuit was used to transform the resistors into sensors, which were then applied to monitor small displacements. This project contributes to the industrial application and commercialization of the bipolar resistance effect in semiconductor materials.

Keywords: lateral bipolar photoresistance effect, photo-varistor, sensor

Contents

1. The Principle of Bipolar Resistance Effect (Reference [2])	3
2. The process and results of the research.	4
2.1 By testing the 14 silicon pieces produced, select silicon piece samples with good linearity for the core components of the variable resistor	4
2.2 Prototype of varistor samples with good linearity and high sensitivity has been produced.	5
2.3 Prototype of a micro displacement monitor has been produced.	5
3. Preparation and testing of silicon piece sample	6
3.1 . Preparation silicon piece sample.	6
3.1.1 Cleaning semiconductor substrate materials	6
3.1.2 Corrosion of semiconductor surfaces.	7
3.1.3 Coating using magnetron sputtering technology	8
3.2 Testing the Resistance Effect of Semiconductor Samples	10
3.2.1 Test Case 1.	11
3.2.2 Test Case 2.	12
3.2.3 Test Case 3.	13
3.2.4 Test Case 4.	14
3.2.5 Test Case 5	14
3.2.6 Test Case 6.	15
3.2.7 Test Case 7.	15
3.2.8 Test Case 8.	16
3.2.9 Test Case 9.	16
3.2.10 Trend analysis and summary	17
4. Making semiconductor variable resistance devices	19
4.1 Production process	19
4.2 Testing of Rheostats	21
4.2.1 A smaller range and lower sensitivity variable resistor (with Sample 12).	21
4.2.2 A large range and high sensitivity variable resistor (with Sample 13)	22
Test Data:	22
5. Application - displacement monitoring sensor based on a new semiconductor optoelectronic variable resistor.	24
6. Reflection on relevant issues and further research	28
6.1 Some details are not handled perfectly	28
6.2 More experiments are needed.	29
6.3 Analysis of newly discovered phenomena	30
Reference	31
Acknowledgements.	32

1. The Principle of Bipolar Resistance Effect (Reference [2])

The photoresistive bipolar resistance effect is a unique phenomenon that exists in specific semiconductor materials. When a laser spot moves along a line segment from one electrode to another, the resistance of the semiconductor exhibits a significant linear change corresponding to the position of the light spot.

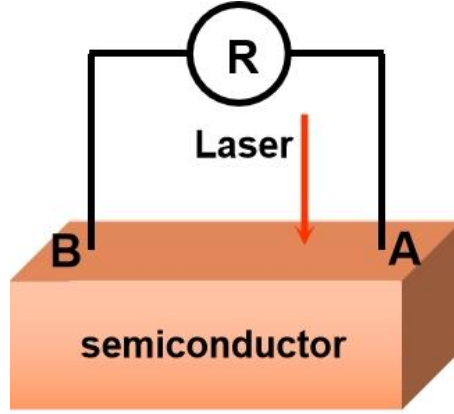


Figure 1. Schematic diagram of bipolar resistance effect, reference [2]

Under laser irradiation, the laser can excite electrons in the semiconductor, with a probability of causing these electrons to transition to the metal layer, followed by diffusion in the metal layer. At the same time, the drifting electrons in the metal layer itself are also moving. Therefore, on the left side of the irradiation point, the diffusing electrons and drifting electrons move in opposite directions, resulting in strong scattering and an increase in resistance, forming a high resistance region. On the right side of the irradiation point, the diffusing electrons and drifting electrons move in the same direction, resulting in a lower resistance. Therefore, by calculating the resistivity at each point on the left side and right side, and performing a definite integral, the resistance at the corresponding position can be obtained. The resistance value of the semiconductor structure under laser irradiation is given by:

$$R(x) = R_0(1 + Kx) \quad (-L < x < L) \quad (1)$$

Here K is the proportion coefficient of the semiconductor structure itself, which is:

$$K = \frac{n_0 e^{-L/l}}{N_0 L} \quad (2)$$

where N_0 is the drift electron concentration, L is the distance from the midpoint to one end of the electrode, l is the electron diffusion length, and n_0 is the electron concentration at the point of laser irradiation.

This also reflects that the change in resistance follows a linear trend.

2. The Process and Results of the Research

Professor Wang Hui's laboratory at Shanghai Jiao Tong University have conducted research on the bipolar resistance effect of various semiconductor materials and mentioned that this effect can be used to create a new type of optically controlled variable resistor. However, further research on the fabrication process of this optically controlled variable resistor has not been conducted. In this paper, I first reproduced the bipolar resistance effect in different semiconductor materials and determined the most suitable material for fabricating the optically controlled variable resistor based on this effect. Finally, I conducted research on the fabrication process of the optically controlled variable resistor using the selected material.

2.1 Fabrication of the 14 type of silicon piece samples

In order to investigate the influence of various semiconductor materials on their resistance effect (mainly including bare silicon, porous silicon, Ag/Si surface silver plated semiconductors, and Ag/SiO₂/Si MOS semiconductor materials), the following 14 types of silicon pieces were prepared for testing:

- (1) P-type bare silicon
- (2) N-type bare silicon
- (3) P-type porous silicon corroded for 5 minutes
- (4) P-type porous silicon corroded for 10 minutes
- (5) N-type porous silicon corroded for 5 minutes
- (6) N-type porous silicon corroded for 10 minutes

- (7) Ag/Si P-type corroded for 5 minutes
- (8) Ag/Si N-type corroded for 5 minutes
- (9) Ag/Si P-type corroded for 10 minutes
- (10) Ag/Si N-type corroded for 10 minutes
- (11) Ag/SiO₂/Si P-type corroded for 5 minutes
- (12) Ag/SiO₂/Si N-type corroded for 5 minutes
- (13) Ag/SiO₂/Si P-type corroded for 10 minutes
- (14) Ag/SiO₂/Si N-type corroded for 10 minutes

It was found that three samples showed good linearity between the two poles, among which sample 13 had the best linearity, Ag/SiO₂/Si P-type silicon corroded for 10 minutes, with a sensitivity of up to 3.08K Ω per millimeter.

Two samples were damaged, and the change in resistance between the two poles of the other samples did not show a significant linear relationship, even non-linear.

2.2 Prototype of varistor samples with good linearity and high sensitivity

Two of the three samples with good linearity were selected as the core components for making a variable resistor. Then I designed other components of the variable resistor, printed them out using a 3D printer, and assembled these components with silicon piece samples for testing. I successfully fabricated two prototype optoelectronic variable resistor samples. One type is a smaller range and lower sensitivity variable resistor (variable resistor with Ag/SiO₂/Si P-type silicon corroded for 10 minutes, the range of 1.3331K Ω -1.95K Ω and the sensitivity of 0.4429 K Ω /mm). Another type is a high-sensitivity variable resistor with a large range (variable resistor with Ag/SiO₂/Si P-type silicon corroded for 10 minutes, the range of 133.31K Ω -149.03K Ω and the sensitivity of 8.274 K Ω /mm).

2.3 Prototype of a micro displacement monitor

Based on the prepared photo controlled variable resistor and the linearization feature of the photo-controlled resistance change, I added an analog-to-digital conversion circuit and conversion algorithm, and completed the complete displacement monitoring sensor sample using Arduino. Due to the small size of the entire device, if industrial packaging is adopted in the future, the integration level can be further improved.

3. Preparation and Testing of Silicon Piece Sample

3.1 Preparation silicon piece sample

The first step of the experiment is to prepare the test sample, prepare porous silicon as the base material, and coat it with a metal film (Ag). The specific sample fabrication process is as follows:

3.1.1 Cleaning semiconductor substrate materials

First, pre-treat the silicon piece by holding a cotton ball with tweezers and dipping it in acetone. Gently wipe the surface of the silicon piece to remove any industrial glue and surface oxide layers. After the pre-treatment, proceed with the actual cleaning process.

The operational steps for cleaning are as follows:

- 1) Pre-treat the surface of the silicon piece using cotton balls soaked in ethanol.
- 2) Place the pre-treated silicon piece into a beaker, add acetone, and perform a 20-minute of ultrasonic cleaning.
- 3) Discard the acetone, pour ethanol into the beaker, and continue with a 20-minute ultrasonic cleaning.

This procedure effectively cleans the silicon pieces, so I proceeded to clean all 14 pieces following the same sequence.

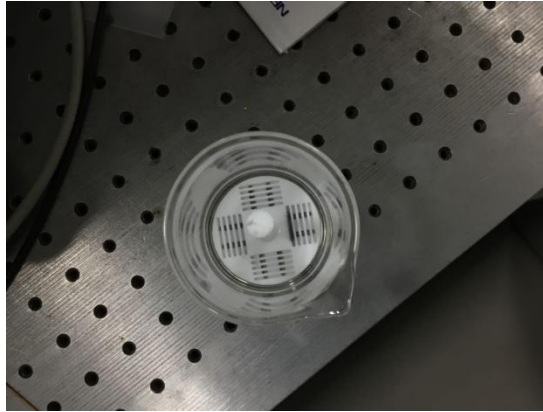


Figure 2: Silicon pieces placed in ethanol

3.1.2 Corrosion of semiconductor surfaces



Figure 3. Corrosion tank for fabricating porous silicon

After the cleaning process, the next step is the corrosion process on the semiconductor surface. Unlike the previous references, this time I started by preparing the corrosion solution. The solution consists of 4g ammonium fluoride, 30mL deionized water, 80mL ethanol, and 70mL phosphoric acid. First, I took the ammonium fluoride out of the freezer and used a spoon to extract the solid form. Then, I added 30mL of deionized water to dissolve the ammonium fluoride (adding deionized water helps to accelerate the dissolution process). After the dissolution, I added ethanol and then phosphoric acid, allowing each component to dissolve completely. Once fully dissolved, I obtained a colorless test reagent.

Next, during the preparation process, I need to pour the reagent into the tank shown in Figure 3. Insert a graphite sheet at one end and connect the wire to serve as the cathode. On the other end, use a metal clip with wires to clamp the semiconductor

sample and insert 1/3 of the sample into the reagent as the anode. This step aims to corrode the surface of silicon pieces and create porous silicon structures through the ionization process. During the ionization process, I was able to control the output voltage. In this experiment, the current was controlled at 0.1A by adjusting the voltage, and two types of silicon pieces were successfully made, one for corrosion for 5 minutes and the other for corrosion for 10 minutes. Interestingly, I observed that P-type silicon usually required a longer time to reach the 0.1A current output in the device, while N-type silicon typically exhibited the 0.1A current output immediately upon applying the voltage. This finding is quite remarkable and may be related to the material properties.

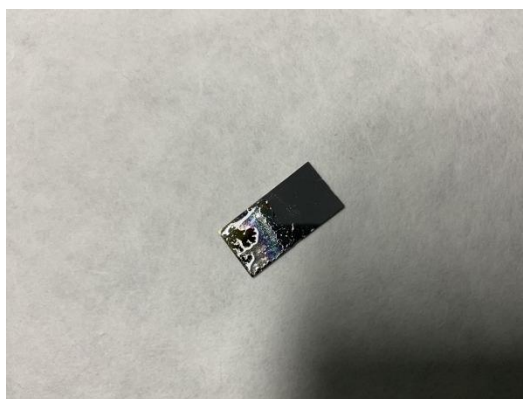


Figure 4: Semiconductor silicon pieces that have not been blown dry after corrosion

3.1.3 Coating using magnetron sputtering technology

The next step involves using DC magnetron sputtering for coating, which is one of the advanced techniques currently used for depositing metal films on semiconductor surfaces. This technique offers several advantages, including low substrate surface temperature, high coating efficiency, and uniform film thickness. The main principle of this coating process is to accelerate the metal target material, such as argon ions, towards the target material using inert gas ions. The accelerated ions bombard the negatively charged target material, causing atoms to be ejected from its surface, resulting in sputtering. The coating steps are as follows:

Power on:

- (1) Turn on the main power supply.

- (2) Turn on the power to the water pump.
- (3) Turn on the mechanical pump and low vacuum gauge.
- (4) Slowly open V6 and close it after the pressure drops to 20pa.
- (5) Turn on the solenoid valve and turn on the molecular pump.
- (6) Open the gate valve.

Sputtering:

- (1) Close the ionization gauge.
- (2) Open the intake valves (V4, V5).
- (3) When the pressure reaches $9 * 10^{-4}$ pa, close the gate valve.
- (4) Open the pressure reducing valve at the bottle and then turn on the volumetric flow meter.
- (5) Adjust the gate valve to maintain a constant air pressure of 0.7pa.
- (6) Turn on the DC power supply for sputtering.
- (7) Rotate the corresponding position between the substrate and the target material to control the time.

The distance between the target housing and the target material is 2-3mm, and they must never come into contact to avoid short circuits.

The sequence for operating the molecular pump:

- first, turn on the on/off button,
- set the FUNC DATA button to zero,
- and then press the START button.

Detailed steps for sputtering:

- After the pressure drops to $5 * 10^{-4}$ pa, close the pressure reducing valve at the gas cylinder.
- Power supply to gas flow meters.
- Turn off the high vacuum gauge and open the argon intake valve.
- Set the gas flow meter to the degassing (cleaning) position.
- After the pressure drops to 10^{-1} pa, turn on the high vacuum gauge.
- After the pressure drops to 10^{-4} pa, turn the gas flow meter to the closed position (close the high vacuum gauge).
- Adjust the pressure reducing valve of the gas cylinder (0.1-0.15Mpa).
- Set the gas flow meter to the valve control position and adjust the flow rate (10-13).
- Close the gate valve to a certain extent.

In addition, it is necessary to control the sputtering time. In this experiment, the sputtering time for the Ag film is 8 seconds, while the sputtering time for the SiO₂ oxide layer is approximately one minute. These values are based on empirical knowledge obtained by consulting other members of the laboratory. Furthermore, during the sputtering process, the target is moved using a computer program.

For this project, 14 semiconductor silicon pieces were prepared. In the first step, pieces numbered 1 to 14 were cleaned, with samples 1 and 2 used as control benchmarks. In the second step, pieces numbered 3 to 14 (a total of 12 pieces) underwent a 5-minute or 10-minute corrosion. In the third step, different metal films were deposited on pieces numbered 7 to 14 (a total of 8 pieces).

As a result, 14 semiconductor pieces with different structures were prepared as listed before.

3.2 Testing the Resistance Effect of Semiconductor Samples

After preparing all 14 semiconductor structures, I proceeded to set up the apparatus to measure the bipolar resistance effect of each silicon piece. I used a laser with a specific wavelength to test the sensitivity of the samples to different power levels. The experimental method is as follows: the laser is moved using a precision slide stage, and the changes in electron diffusion length and resistance for each sample are recorded.

To begin the experimental procedure, the semiconductor samples need to be connected to electrodes. In this case, I chose to use indium. I cut a small piece of indium from the existing indium wire and used a toothpick to attach it to the semiconductor sample, ensuring that the distance between the two indium points is not too far apart. Then, I prepared a copper wire that can conduct electricity and pressed it onto the indium point. Next, I cut two more pieces of indium and pressed them onto the copper wire, effectively sandwiching the two copper wires and creating two electrodes. Finally, I connected the copper wires to the circuit of a multimeter instrument used for resistance measurement, as shown in Figure 5.

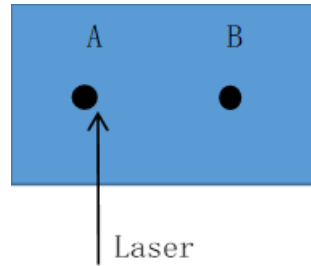


Figure 5. Diagram of the testing

Where the blue rectangle represents the semiconductor sample, the arrow represents the beam of the laser, and the two dots represent the two electrodes. The laser moves from point A to point B along the AB line segment, and the changes in resistance are recorded.

The overall device is shown in Figure 6:

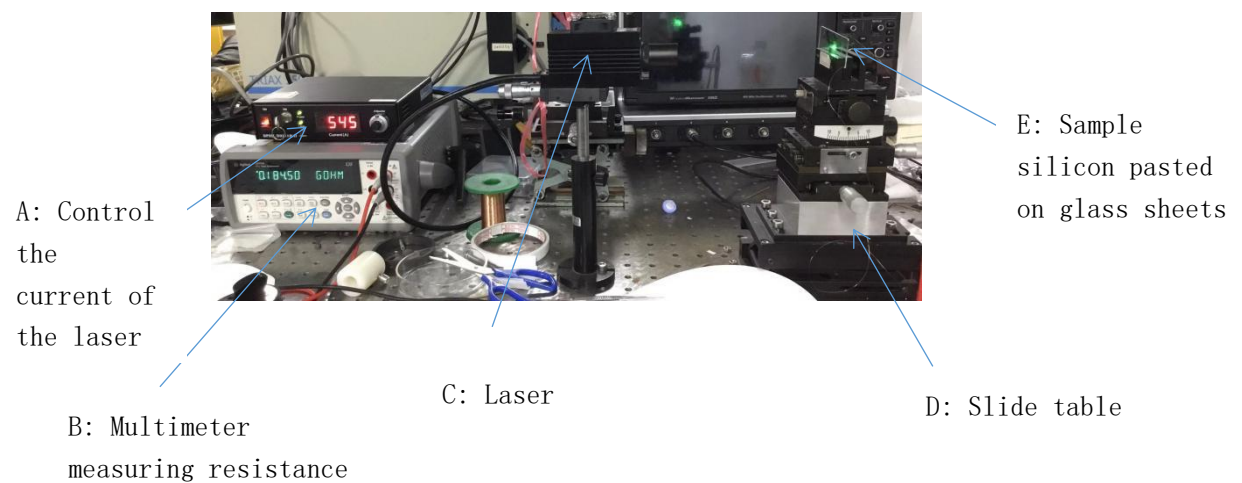


Figure 6. Experimental equipment

I conducted a total of 9 tests, and for each test, data measurements were taken, graphs were plotted, and patterns were analyzed. Finally, I summarized all the tests using a table and provided a conclusion.

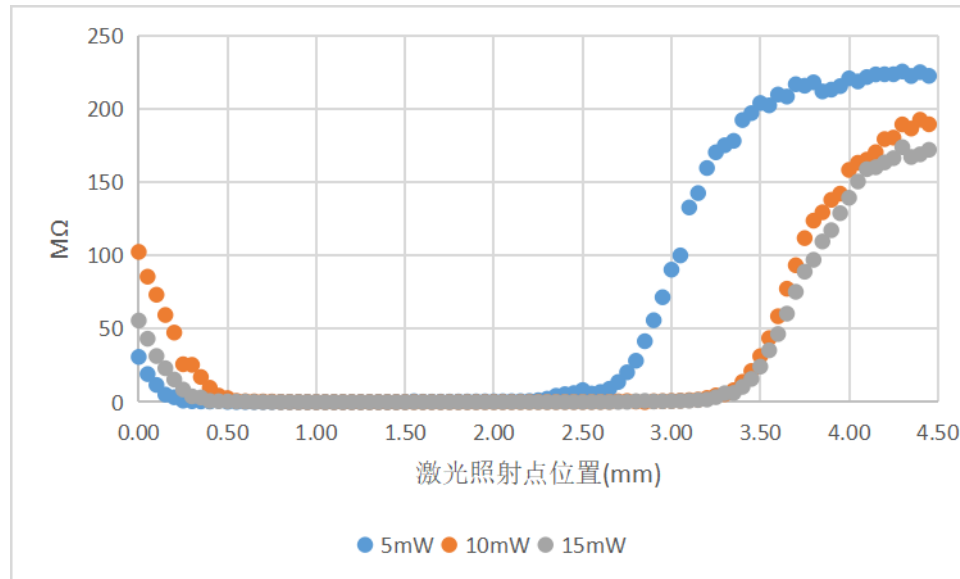
3.2.1 Test Case 1

Time: December 9, 2021, 16:30-21:00 PM

Number: Sample 4 (Porous P-type silicon corroded for 10 minutes)

Electrode position: 0.5mm to 2.5mm.

Purpose: To measure the effect of different laser powers on resistance sensitivity under the same material, the measured data are as follows:



From the experimental results, it can be seen that the resistance change caused by the displacement of the laser between the two electrodes is not significant. This is likely due to the large distance between the two electrodes, which did not meet the requirement of being much smaller than the electron diffusion length. Based on Yu Chongqi's paper [2], as the laser power increases, the sensitivity also increases accordingly, but after reaching a certain level (about 10mW), the sensitivity change is not significant. Therefore, in order to reduce the impact of laser power on the test results, the laser power used in subsequent tests of this study was 15mW.

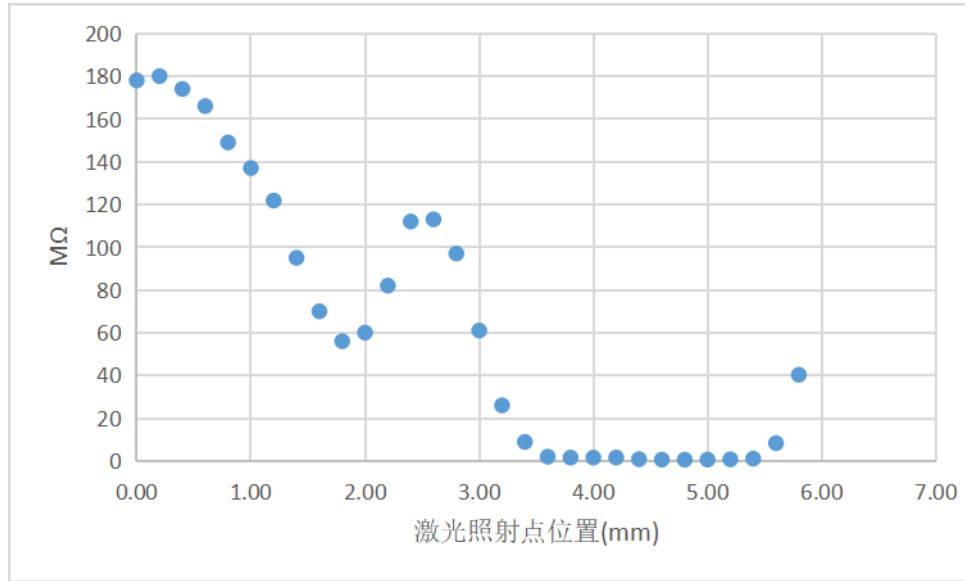
3.2.2 Test Case 2

Time: December 9, 2021, 16:30-21:00 PM

Number: Sample 1 (P-type bare silicon)

Electrode positions: 0.8mm and 3.2mm.

Purpose: To measure the bipolar resistance effect of this structure. Obtain the following data:



This experiment discovered a non-linear increase in resistance at the midpoint as the irradiation point moved upward. **This phenomenon, which deviates from linearity, has not been mentioned in previous literature.**

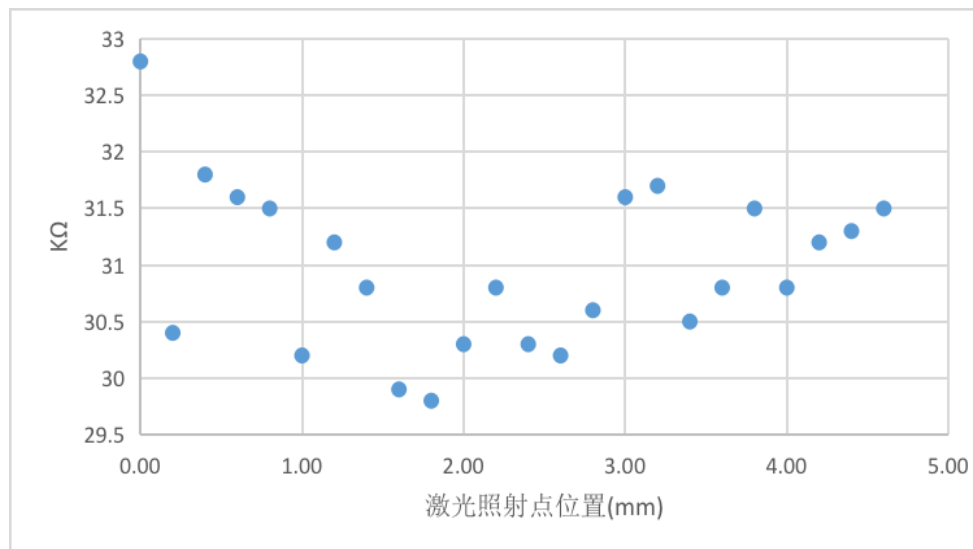
3.2.3 Test Case 3

Time: December 9, 2021, 16:30-21:00 PM

Number: Sample 2 (N-type bare silicon)

Electrode positions: 1mm and 3mm.

Purpose: To measure the bipolar resistance effect of this structure. Obtain the following data:



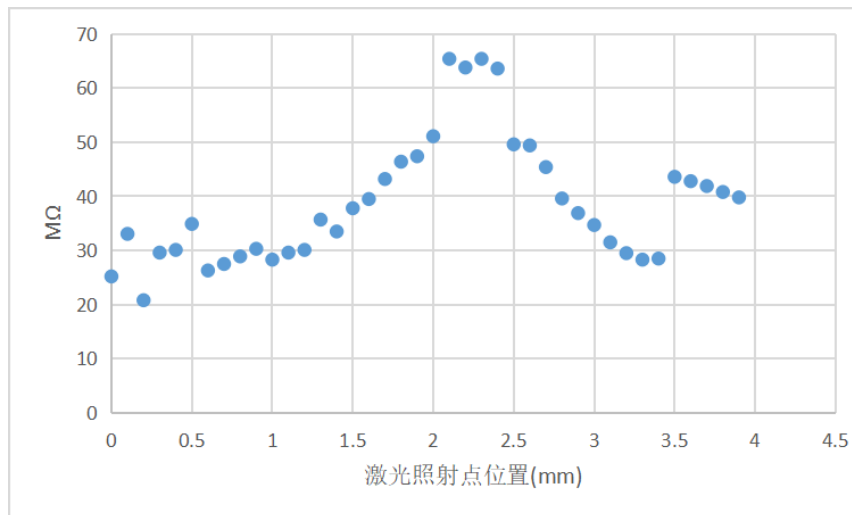
3.2.4 Test Case 4

Time: December 9, 2021, 16:30-21:00 PM

Number: Sample 7 (P-type silicon of Ag/Si corroded for 5 minutes)

Electrode positions: 1.5mm and 3mm.

Purpose: To measure the bipolar resistance effect of this structure. Obtain the following data:

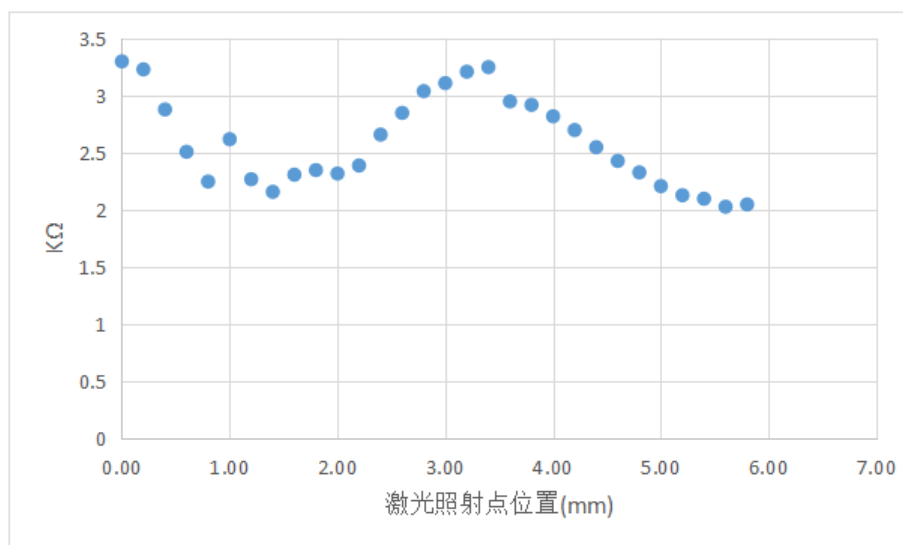


3.2.5 Test Case 5

Time: December 9, 2021, 16:30-21:00 PM

Number: Sample 8 (N-type silicon of Ag/Si corroded for 5 minutes)

Electrode positions: 2mm and 3.5mm.

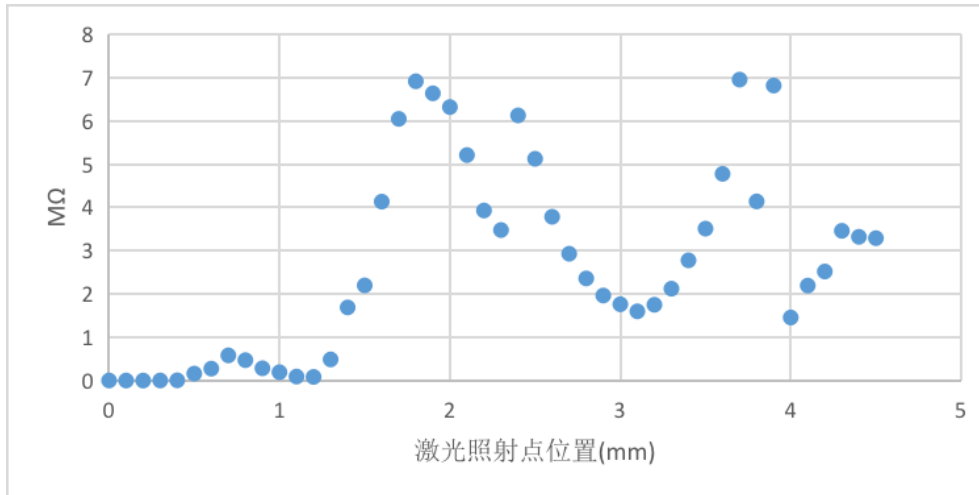


3.2.6 Test Case 6

Time: December 10, 2021, 4:00 PM -20:00 PM

Number: Sample 9 (P-type silicon of Ag/Si corroded for 10 minutes)

Electrode positions: 1.3mm and 3mm.



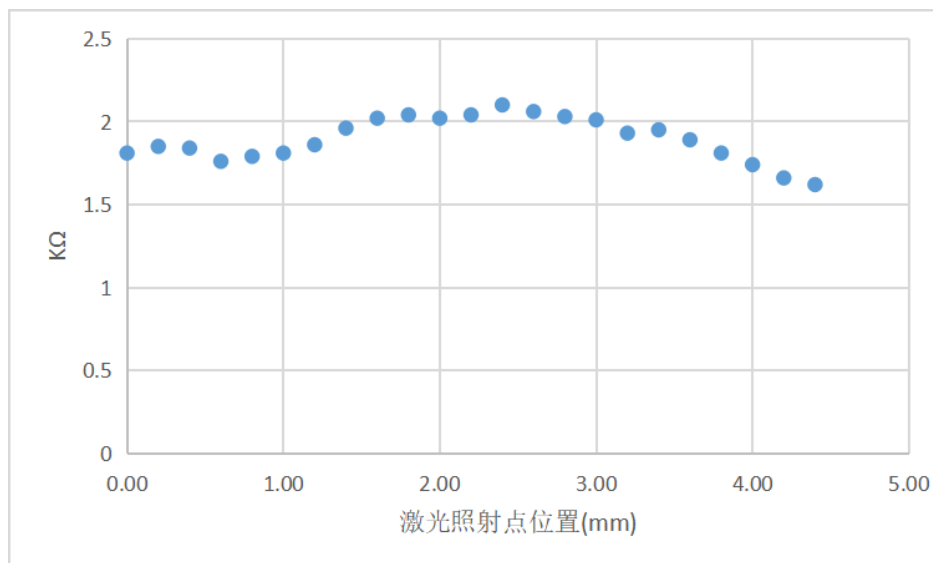
3.2.7 Test Case 7

Time: December 10, 2021, 4:00 PM -20:00 PM

Number: Sample 10 (N-type silicon of Ag/Si corroded for 10 minutes)

Electrode position: Place the electrodes at 0mm and 2mm positions.

Purpose: To measure the bipolar resistance effect of this structure. Obtain the following data:



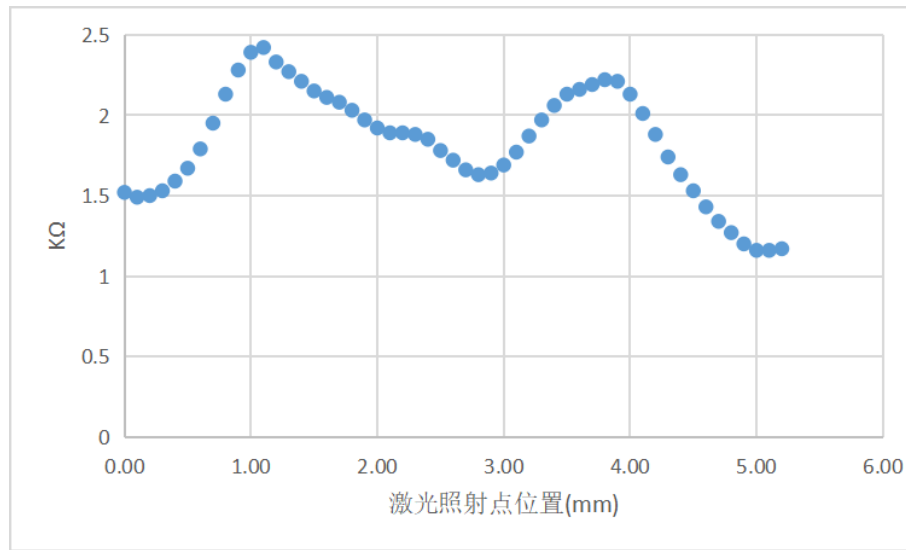
3.2.8 Test Case 8

Time: December 10, 2021, 4:00 PM -20:00 PM

Number: Sample 12 (N-type Ag/SiO₂/Si)

Electrode positions: 1mm and 2.8mm.

Purpose: To measure the bipolar resistance effect of this MOS structure. Obtain the following data:



In this MOS structure, a strong linear variation was observed between the two electrodes. However, it is interesting to note that there is a small portion of nonlinear region between 2.1mm and 2.3mm in the middle, which is likely caused by a larger electrode distance of 1.8mm. The remaining parts follow the same pattern as obtained from reference [2].

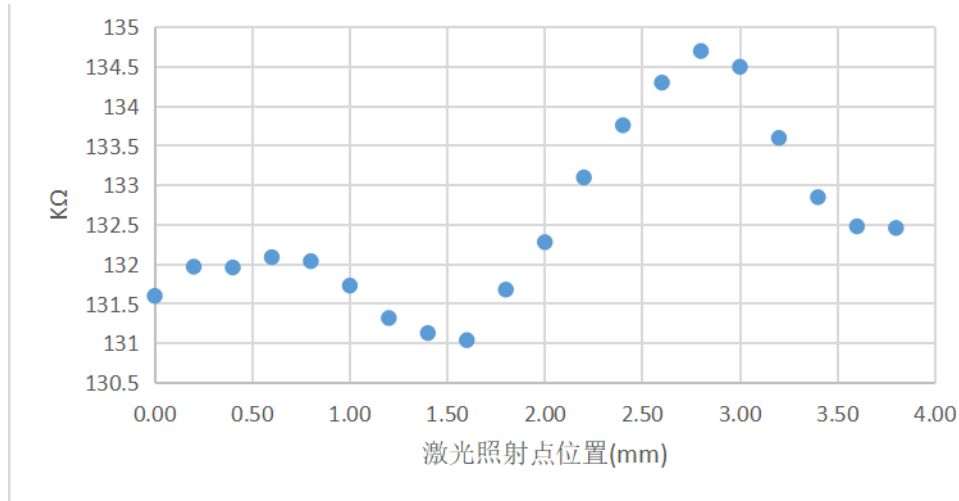
3.2.9 Test Case 9

Time: December 10, 2021, 4:00 PM -20:00 PM

Number: Sample 13 (Ag/SiO₂/Si P-type silicon corroded for 10 minutes)

Electrode position: The electrodes are installed at 1.5mm and 2.8mm positions.

Purpose: To measure the bipolar resistance effect of this MOS structure. Obtain the following data:



Analysis: In the P-type silicon structure of Ag/SiO₂/Si corroded for 10 minutes, strong linearity was found, and its sensitivity was also higher than that of the Ag/SiO₂/Si N-type silicon structure corroded for 10 minutes. The strong linearity of MOS structures is likely due to their longer diffusion length, so as shown in formula (2), the resistance change at an electrode distance of about 1.5mm-2mm can be better approximated as linear compared to other structures. However, due to the smaller diffusion length of other structures, the diffusion of charge carriers to another electrode causes nonlinear resistance changes. Secondly, this experiment shows that the variation of N-type bare silicon is smaller than that of P-type silicon, and there is no linear relationship, which is also an issue not discussed in the references.

There is contamination on the surface of samples 11 and 14 due to improper experimental operations, and some of the surface coatings are damaged, so no measurements were taken.

3.2.10 Trend analysis and summary

Test No.	Sample No.	Electrode position	Analysis
1	Sample 4 P-type porous silicon corroded for 10 minutes	0.5mm, 2.5mm	The resistance change caused by the displacement of the laser between the two electrodes is not significant. This may be due to the large distance between the two electrodes, which did not meet the requirement of being much smaller than the electron diffusion length. From the results, it cannot be distinguished which power has the greatest sensitivity change on semiconductor samples.

2	Sample 1 P-type bare silicon	0.8mm, 3.2mm	This experiment found that the resistance increases linearly with the displacement of the irradiation point in the middle, which does not conform to the linear situation. This situation has not been mentioned in previous published papers.
3	Sample 2 N-type bare silicon	1mm, 3mm	This experiment found that the variation of this N-type bare silicon is minimal and has no linear relationship, presenting an overall nonlinear region. This may be because the position of the silicon piece during measurement is a bit crooked, so the path of the laser does not match the line segment formed by the two electrodes, or it may be because in bare silicon, the bipolar resistance effect itself is not strong.
4	Sample 7 Ag/Si P-type corroded for 5 minutes	1.5mm, 3mm	There is no basic coherent linear trend here, but rather a linear increase followed by a non-linear zone before a linear decrease. Although it basically conforms to a linear relationship, it does not show a trend of continuous increase or decrease. In summary, this time there was an intention to reduce the distance between the two electrodes, but there was still no linear relationship, possibly because the distance between the two electrodes was still too large.
5	Sample 8 Ag/Si N-type corroded for 5 minutes	2mm, 3.5mm	Although the distance between the two electrodes was not reduced, a basically linear increasing line can still be observed.
6	Sample 9 Ag/Si P-type corroded for 10 minutes	1.3mm, 3mm	This time, after the initial linear growth, it showed a non-linear region similar to Ag/Si silicon pieces, followed by a linear decrease.
7	Sample 10 Ag/Si N-type corroded for 10 minutes	0mm, 2mm	Although there is a certain linear upward trend in resistance, the overall resistance does not change much.
8	Sample 12 Ag/SiO ₂ /Si N-type corroded for 5 minutes	1mm, 2.8mm	In this metal oxide semiconductor structure, a strong linear variation was observed between the two electrodes. However, it is interesting to note that there is a small portion of nonlinear region between 2.1mm and 2.3mm in the middle, which is likely caused by a larger electrode distance of 1.8mm.
9	Sample 13 Ag/SiO ₂ /Si P-type corroded for 10 minutes	1.5mm, 2.8mm	In the P-type silicon structure of Ag/SiO ₂ /Si corroded for 10 minutes, strong linearity was found, and its sensitivity was also higher than that of the Ag/SiO ₂ /Si N-type silicon structure corroded for 10 minutes.

From the above test results, I found a good linear relationship in the resistance between the two electrodes in samples 8, 12, and 13.

In the future, I will use the three samples obtained above that meet the sensitivity requirements as basic components to make a variable resistor.

4. Making Semiconductor Variable Resistance Devices

4.1 Production process

In order to create a portable and compact variable resistor, I decided not to use the multifunctional, large-sized, and expensive laser available in the laboratory. Instead, I purchased a batch of small lasers with the same wavelength as those used in the lab. These lasers have a head diameter of only 1 centimeter and a length of 2.6 centimeters. Additionally, to streamline the equipment, I acquired a small precision slide stage. The use of these compact devices aims to improve portability, reduce costs, and allow me to conduct experiments in smaller spaces.

To connect the slide stage with the semiconductor sample, I designed the following 3D artifact and used a 3D printer for its production. This artifact is 63mm long, 50mm wide, and 43mm high. As shown in Figure 7:

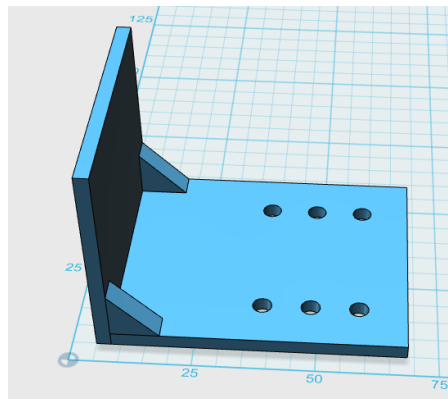


Figure 7. 3D model of the stand

In order to connect the slide stage and laser, I also designed another 3D artifact, which is 40mm long, 30mm wide, and 3mm thick, as shown in Figure 8:

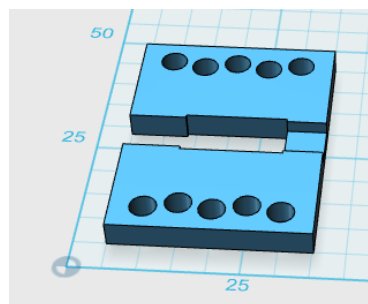


Figure 8. 3D model of laser mounted board

During the manufacturing process, I encountered an issue regarding how to secure the silicon piece. Due to the silicon piece's extreme fragility and its inability to be exposed to air for extended periods, as well as the need for delicate manipulation using tweezers, I needed to find a way to stabilize both the silicon piece and the copper wire. My solution was to sandwich the silicon piece and the copper wire between two cleaned glass slides. This approach ensures that the laser can irradiate the sample without obstruction while also securely holding it in place.

Here's how the operation is carried out: Firstly, place one sample on a glass slide, and after clamping the copper wire with indium dots, use tape to secure the copper wire, ensuring it remains in place during the process. Then, cover the sample with a second glass slide and use adhesive to bond the two glass slides together (taking care to ensure the adhesive does not come into contact with the semiconductor). Please refer to Figure 9 for a visual representation.:

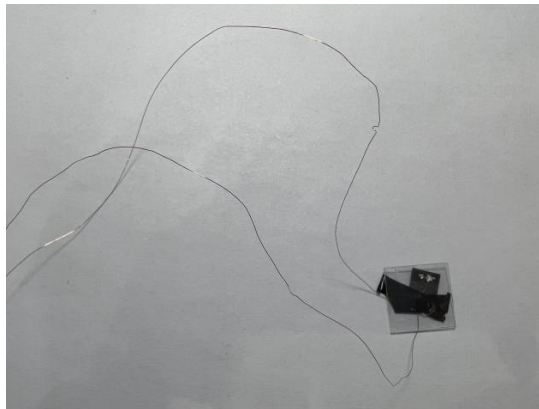


Figure 9. a silicon piece fixed with glass sheets

The solution mentioned above is just a sample setup. After consulting the information, I believe that for further development, an industrial packaging with a glass window can be used. This not only provides better stability but also allows for further size reduction.

By connecting all the components together, the preliminary form of the semiconductor resistive sensor device is completed, as shown in Figure 10:

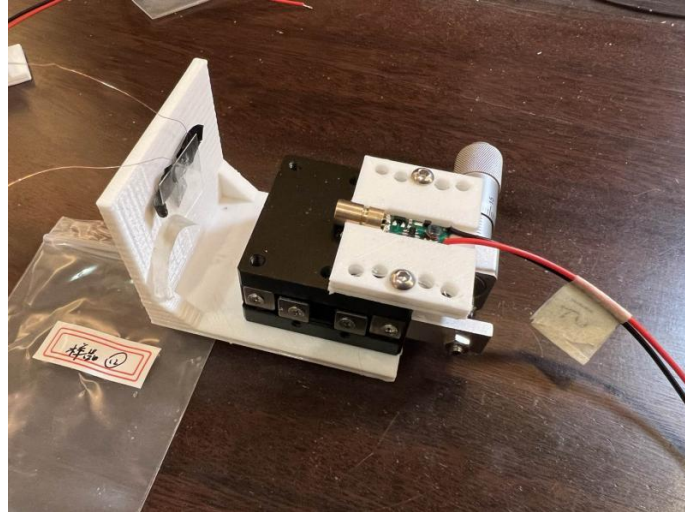


Figure 10. Prototype of Semiconductor Rheostat

4.2 Testing of Rheostats

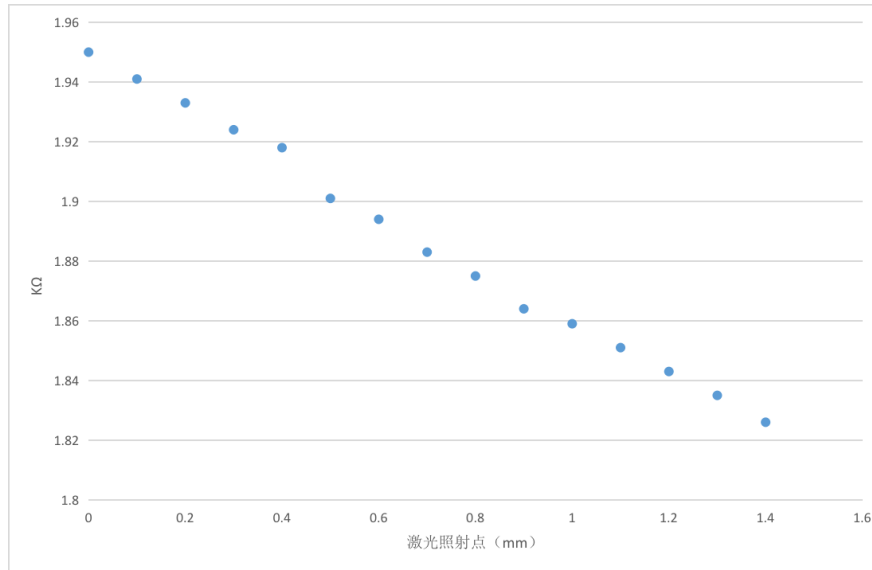
After testing sample 12 and sample 13 separately, two types of varistors with different ranges and sensitivities were produced, one with lower sensitivity for a smaller range and the other with higher sensitivity for a larger range.

4.2.1 A smaller range and lower sensitivity variable resistor (with Sample 12)

Test data:

Laser point position	Resistance value (K Ω)
0	1.95
0.1	1.941
0.2	1.933
0.3	1.924
0.4	1.918
0.5	1.901
0.6	1.894
0.7	1.883
0.8	1.875

0.9	1.864
1	1.859
1.1	1.851
1.2	1.843
1.3	1.835
1.4	1.826



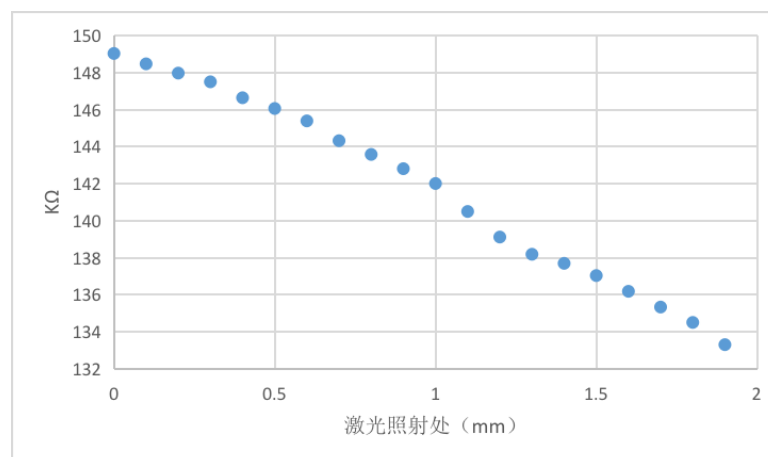
In order to improve the linearity, I reduced the distance between the two electrodes. As shown in the above test results, the linearity is indeed good, and some nonlinear regions that were originally present have now disappeared. The two electrode positions used here are 0mm and 1.4mm respectively. The resistance range of this Ag/SiO₂/Si P-type silicon structure corroded for 10 minutes is 1.33K Ω -1.95K Ω , with a sensitivity of 0.44K Ω /mm.

4.2.2 A large range and high sensitivity variable resistor (with Sample 13)

Test Data:

Laser point position	Resistance value (K Ω)
----------------------	--------------------------------

0	149.03
0.1	148.47
0.2	147.97
0.3	147.5
0.4	146.64
0.5	146.06
0.6	145.39
0.7	144.32
0.8	143.58
0.9	142.81
1	142.01
1.1	140.5
1.2	139.12
1.3	138.19
1.4	137.7
1.5	137.04
1.6	136.19
1.7	135.34
1.8	134.51
1.9	133.31



The two electrodes of the Ag/SiO₂/Si P-type silicon structure, which were corroded for 10 minutes, were located at 0mm and 1.9mm, respectively. The resistance range was 133.31K Ω -149.03K Ω , and the sensitivity was 8.27K Ω /mm.

From the experimental results, it can be observed that the glass cover of the device does not affect the power of laser irradiation and has no impact on the bipolar resistive effect of the sample.

5. Application - displacement monitoring sensor based on a new semiconductor optoelectronic variable resistor

Based on the high sensitivity and wide linear range of the optical control resistive sensor, which is based on the laser spot irradiation position, it can be applied to the monitoring of small displacements and developed into a sensor for detecting small displacements. It can be used for detecting physical dimensional variations, thereby finding extensive application in tolerance quality control of precision devices. It can also be used for monitoring mechanical displacements in various fields where small displacements occur due to stress, mechanical vibrations, and other factors.

I plan to add an analog-to-digital conversion circuit to further automate the displacement control.

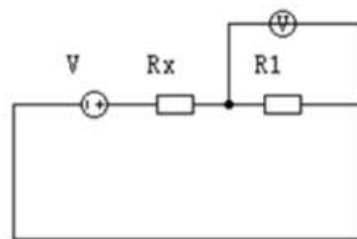


Figure 11. Resistance voltage divider circuit diagram

where V represents the total voltage, while Rx here is the resistance value of the photoelectric variable resistor that I need to obtain, and R1 is a set resistance value. By measuring the voltage value of R1, the resistance value of Rx can be obtained. The expression is:

$$R_x = \frac{R_1(V - V_1)}{V_1} \quad (3)$$

Based on the high resistance value of the optical control resistive sensor produced in this project, it can be easily read using the analog pins of Arduino, making it cost-effective. By utilizing the slope parameters calibrated from previous experiments with the semiconductor resistive device, it is possible to calculate the relative displacement of the laser spot output.

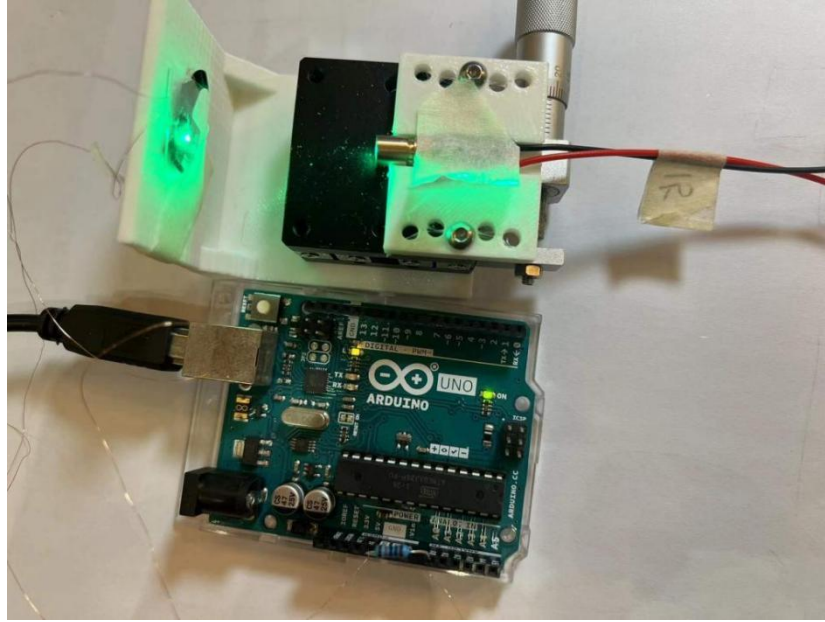


Figure 12. Using Arduino as signal monitoring

Sample 13 (Ag/SiO₂/Si P-type silicon structure corroded for 10 minutes) was used in this experiment. The optimal line was drawn from the linear data in 5.5.2, and the expression for resistance is:

$$R(x) = -8.273684x + 149.03 \quad (0 \leq x \leq 1.9) \quad (4)$$

Where x represents displacement in mm, and R (x) represents resistance in K Ω .

Expression for displacement:

$$x = \frac{(R-149.03)}{-8.273684} \quad (133.31 \leq R \leq 149.03) \quad (5)$$

The code of resistorx() running in Arduino is as follows (calculate the current resistance value of the semiconductor variable resistor based on the measured voltage value):

```
double resistorex(double R1, int V1){
double Rx=0;
if(V1!=0){
Rx = (1023-V1)*R1/V1;
}
return Rx;
}
```

The function resistor2position() calculates the displacement based on the resistance value.

```
double resistor2position(double y){
double x=0;
double a =-8.273684;
double b = 149.03;
x = (y-b)/a;
return x;
}
```

The total voltage I have chosen in this circuit is 5V, and in Arduino, 1023 represents 5V voltage. The input parameters R1 and V also correspond to the formula.

In the loop loop of Arduino, use analogRead() to read the input measurement voltage, and then call the first two functions to calculate the displacement change. The displacement data provided is in millimeters.

```
void setup() {
//Open the serial port connection between the Arduino board and the computer, and
initialize the baud rate with a default of 9600
Serial.begin(9600);
}

void loop() {
// put your main code here, to run repeatedly:
int sValue = analogRead(A0);
Serial.println(sValue);
Serial.println(resistorex(100,sValue));
Serial.println(resistor2position(resistorex(100,sValue)));
}
```

```

delay(1000);
}

```

There are three rows of test data for each group. The first row shows the voltage measured by the voltmeter, which is not measured in volts, but the corresponding value obtained by Arduino after dividing the 5V voltage into 1023 parts. The second line represents the calculated resistance value of Rx, while the third line represents the corresponding displacement.

The screenshot shows the Arduino IDE interface. The sketch editor on the left contains the following code:

```

double resistor2position(double y){
  double x=0;
  double a =-8.273684;
  double b = 149.03;
  x = (y-b)/a;
  return x;
}
double resistorx(double R1, int V){
  double Rx=0;
  if(V!=0){
    Rx = (1024-V)*R1/V;
  }
  return Rx;
}

```

The serial monitor on the right shows the following output:

```

424
141.51
0.91
428
139.25
1.18
428
139.25
1.18
426
140.38
1.05
425
140.94
0.98
422

```

from the serial output of Arduino, the following data can be obtained:

The analog value corresponding to the voltage	Rx (K Ω) Calculated resistance value	Corresponding displacement (mm)
424	141.51	0.91
428	139.25	1.18
428	139.25	1.18
426	140.38	1.05
425	140.94	0.98

Furthermore, I can omit the slide and change the laser point through the deformation of the structural shell, thus achieving the desired monitoring displacement (deformation). At the same time, the Arduino Mini Pro can be used, making the entire device very compact, with a length, width, and height of only 68mm * 28mm * 33mm.

The final monitoring device is shown in Figure 13:

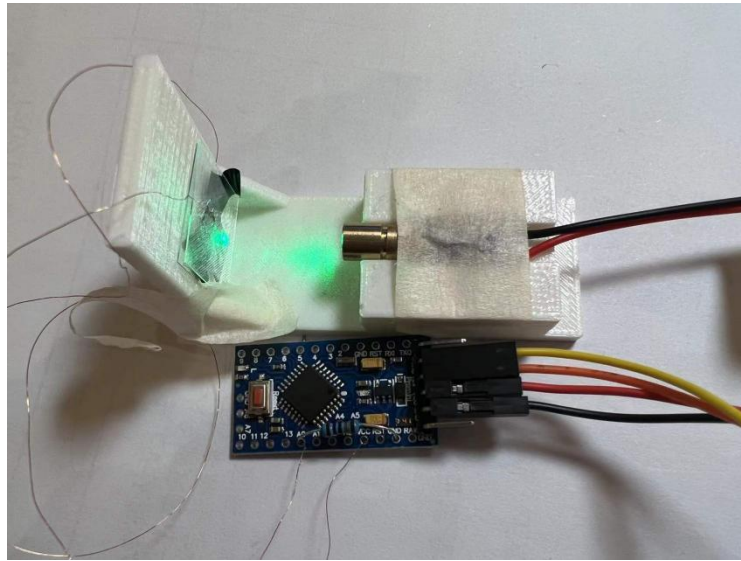


Figure 13. Miniaturized displacement monitoring sensor

6. Reflection on Relevant Issues and Further Research

6.1 Some details are not handled perfectly

The linearity of some samples is not ideal, which may be related to improper handling of certain details during the experimental process. Here are several aspects:

(1) I used copper wires clamped between two small indium dots using toothpicks, which inevitably introduces some errors. For example, during the process of attaching the indium dots, sometimes the dots are made too large. As a result, since the distance between the two electrodes is already approximately 1mm, the large indium dots can cause a narrow region between the electrodes. In other words, although I intended to control the electrode distance to around 1mm, the actual gap in the middle can

sometimes be very small, contributing to the formation of non-linear regions to some extent.

(2) In this project, I did not use a lens combination to focus the laser. Additionally, when the distance between the electrodes is too small, the laser spot often covers both indium dots, leading to a decrease in measurement accuracy and a decrease in linearity.

(3) During the placement of the sample for measurement, sometimes the two electrodes and the plane of laser movement are not on the same level. In other words, the sample is sometimes placed at an angle, which also contributes to the formation of non-linear regions to some extent.

I will address these issues and make improvements in future experiments.

6.2 More experiments are needed

Currently, it is not possible to reliably produce silicon piece samples with specified range and sensitivity. Each time, it needs to be determined through experimental measurements. In the future, I plan to conduct refined experimental operations to make the resistive variation range of the semiconductor structure exhibiting the bipolar resistive effect controllable. These refined experiments will include:

- (1) Testing the influence of different film thicknesses on the resistive effect.
- (2) Modifying the pore size of the porous silicon to adjust the substrate resistance and testing its corresponding resistive effect.
- (3) Testing the influence of different temperatures on the resistive effect.
- (4) Testing the influence of different laser powers on the resistive effect.
- (5) Adding a lens to further adjust the size of the laser spot irradiation to be as small as possible, thereby improving linearity.

It can be expected that after obtaining the data from these experiments, it will be possible to optimize a series of silicon pieces with good linearity and high sensitivity. The linearity and sensitivity can be controlled, providing a basis for future large-scale production.

6.3 Analysis of newly discovered phenomena

During the testing of the bare silicon and sample 4, it was observed that the resistance in the intermediate region between the two electrodes remained relatively constant, while there was a certain linear pattern when the laser spot moved outward from the electrodes. This is an issue worth analyzing and will be the main focus of my next research.

Reference

- [1] C. Q. Yu and H. Wang, Sensors 10, 10155-10180 (2010). “Large lateral photovoltaic effect in metal-(oxide-)semiconductor structures”
- [2] Yu Chongqi, New Optoelectronic Effects in Metal (- Oxide) Semiconductor Structures, Master's Thesis, Shanghai Jiao Tong University, 2011
- [3] Li Xiulin,&Chen Peng Ag/bifeo_ (3) Research on the switching characteristics of optoelectronic resistors in/cofeb/ito thin film devices Science and Technology Innovation (11), 2
- [4] Zhang Biao The study of lateral photovoltaic effect and bipolar resistance effect in Cu₂O/Si structure Master's Thesis from Shanghai Jiao Tong University, February 2014
- [5] Semiconductor Physics (7th Edition), The Physics of Semiconductors 7th Edition, edited by Liu Enke, Zhu Bingsheng, and Luo Shengsheng, published by China Industry and Information Technology Publishing Group and Electronic Industry Press
- [6] Optics, edited by Zhao Kaihua, first edition in November 2004, Higher Education Press
- [7] University Physics, with modern physics, Fifteenth Edition, Sears & Zemansky's
- [8] www.mouser.com, the website of Mouser electronics, Inc.
- [9] C. Q. Yu, H. Wang, and Y. X. Xia, Appl. Phys. Lett. 95, 141112 (2009). “Giant lateral photovoltaic effect observed in TiO₂ dusted metal-semiconductor structure of Ti/TiO₂/Si”.

Acknowledgements

During the research process, I received great support and assistance. I would like to express my sincere gratitude to them here. First of all, I would like to express my gratitude to my teacher Zou Juanjuan for her guidance in electromagnetics and semiconductor theory, guiding me to extensively search and consult relevant works of predecessors, refine research directions, and clarify research objects. Require me to approach every step of research with a rigorous and scientific attitude. At the same time, I would like to express my gratitude to Professor Wang Hui from Shanghai Jiao Tong University. Professor Wang Hui has provided great assistance in research equipment and experimental guidance, as well as valuable writing guidance and revision suggestions for this project's paper. I want to thank my parents for providing me with a relaxed growth environment since I was young, which has cultivated my hands-on ability and curiosity about the world. Finally, I would like to thank myself for the twists and turns in the research process, for not giving up, and for my passion for physics research.